

A quick method to identify secular resonances in multi-planet systems with a binary companion

E. Pilat-Lohinger, A. Bazsó

and

B. Funk

Institute for Astronomy, University of Vienna, Türkenschanzstrasse 17, A-1180 Vienna,
Austria

Received _____; accepted _____

ABSTRACT

Gravitational perturbations in multi-planet systems caused by an accompanying star are the subject of this investigation. Our dynamical model is based on the binary star HD41004 AB where a giant planet orbits HD41004 A. We modify the orbital parameters of this system and analyze the motion of a hypothetical test-planet surrounding HD41004 A on an interior orbit to the detected giant planet. Our numerical computations indicate perturbations due to mean motion and secular resonances. The locations of these resonances are usually connected to high eccentricity and highly inclined motion depending strongly on the binary-planet architecture. As the positions of mean motion resonances can easily be determined, the main purpose of this study is to present a new semi-analytical method to determine the location of a secular resonance without huge computational effort.

Subject headings: Dynamical stability – terrestrial-like planets – habitable zones – HD41004 AB

1. Introduction

Detections of planets in binary star systems (see e.g. Roell et al. 2012) and the knowledge that such stellar systems are quite numerous in the solar neighborhood (Duquennoy & Mayor 1991; Raghavan et al. 2010; Tokovinin 2014) have encouraged astronomers to study the planetary motion in such systems. In this context, we have to distinguish different types of motion (Dvorak 1984): (i) the circumstellar or S-type orbits where the planet moves around one stellar component and (ii) the circumbinary or P-type motion where the planetary orbit surrounds both stars. For completeness we mention a third type, known as L- or T-type (or Trojan motion), where the planet moves in the same orbit as the secondary star but 60° ahead or behind the secondary. A restriction in the mass-ratio makes this motion less interesting for binary stars.

Even though it was questionable that planets could exist in binary star systems (especially in tight systems), scientists working in dynamical astronomy have shown very early that planetary motion in binary star systems could be possible in spite of the gravitational perturbations of the second star. Such studies have been carried out long before the detection of planets outside the solar system (see e.g. Harrington 1977; Graziani & Black 1981; Black 1982; Dvorak 1984, 1986; Rabl & Dvorak 1988; Dvorak et al. 1989) and various studies by Benest between 1988 and 1993. The discoveries of a planet in the γ Cephei system (Cochran et al. 2002) and in the Gliese 86 system (Queloz et al. 2000), respectively led to a re-processing of such stability studies (Holman & Wiegert 1999; Pilat-Lohinger & Dvorak 2002; Pilat-Lohinger et al. 2003). Meanwhile about 80 binary star systems are known to host one or several planets¹ and most of them are in circumstellar motion.

However, the studies cited above provide only stability limits for a single planet in a binary

¹see <http://www.univie.ac.at/adg/schwarz/multiple.html> (A binary catalogue of exoplanets maintained by R. Schwarz).

star system. In this study, we investigate the circumstellar motion of two planets and analyze the perturbations caused by the secondary star. Our investigation is based on the work by Pilat-Lohinger (2005) where the influence of a secondary star on two-planets has been studied for the two spectroscopic binaries γ Cephei and HD41004 AB. In both systems, the secondary star is a M-dwarf in a distance of about 20 au from the host-star of the detected gas giant. The numerical study by Pilat-Lohinger (2005) showed significant deviations in the stability maps of a certain area in the two binary systems due to different masses of the host-stars and the discovered planets and the different positions of the latter. A variation of the giant-planet’s semi-major axis provided a first explanation for these deviations.

In the present investigation, we studied the locations of gravitational perturbations² like mean motion resonances (MMRs) and secular resonances (SRs) in the binary system HD41004 AB using numerical computations, taking into account different binary-planet configurations for which we varied (i) the mass of the secondary star and (ii) the eccentricities of the binary star and the detected giant planet. For these configurations, we calculated stability maps for the motion of test-planets orbiting the host-star interior to the giant planet. The numerical results led us to study the planetary motion in detail using a frequency analysis for planar orbits. Moreover, as an experiment we calculated the proper frequencies of the test-planets using the Laplace-Lagrange secular perturbation theory which resulted in a new semi-analytical approach that permits a fast determination of the location of a linear SR. The SR is a striking feature in many dynamical maps in our study and might be important for habitability studies of such systems.

This article is structured as follows: in section 2, we explain the dynamical model and

²We did not study planetary migration in this investigation since we assumed that the formation process was already completed.

initial conditions for the computations and we discuss the perturbations on the planetary motion. Section 3 shows the numerical results for different binary-planet configurations for which we analyze the behavior and the perturbations on the motion of the test-planets. In section 4, we present a new semi-analytical approach to determine the location of the secular perturbation and an application of our method to different binary stars-planet configurations of HD41004 AB. Then we compare the results with those of the numerical study and finally, in section 5 we summarize our study.

2. Numerical computations

Table 1: Initial conditions for the computations (heliocentric – i.e. with respect to m_1):

masses: m_1, m_2 [m_{Sun}] m_3, m_4 [m_{Jup}]	semi-major axis (a) [AU]	eccentricity (e)	inclination (i), argument of perihelion (ω) node (Ω), mean anomaly (M)
$m_1 = 0.7$			
$m_2 = 0.4/0.7/1.0/1.3$	$10 - 50$ $\Delta a = 10$	$0.0 - 0.6$ $\Delta e = 0.2$	$i_2, \omega_2, \Omega_2, M_2 = 0$
$m_3 = 2.5$	1.64	0.2, 0.4	$i_3, \omega_3, \Omega_3, M_3 = 0$
$m_4 = 0.0$	0.15 – 1.3	0.0	$i_4, \omega_4, \Omega_4, M_4 = 0$

For our numerical study of circumstellar motion of two planets in a binary star system we used a configuration resembling the HD41004 AB system where a giant planet has been discovered (Zucker et al. 2003, 2004). This tight binary star is about 43 pc away from our sun. Both stellar components, a K2V and a M2V star, are accompanied by either a giant planet or a brown dwarf, where the latter is ignored in our dynamical model. The parameters of the two stars were taken from the paper by Roell et al. (2012), where the two stellar masses are $0.7 M_{Sun}$ and $0.42 M_{Sun}$, respectively. While the distance of the two

stars seems to be well determined with about 20 au, the binary’s eccentricity is not known³ and needs further observations. The detected giant planet surrounds HD41004A at 1.64 au, well inside the stable area for $e_B = 0.4$ is 2.8 au⁴. And the additional hypothetical test-planet was placed internal to the giant planet in an initially circular orbit. In order to save computation time we used the restricted four body problem where the test-planet has a negligible mass compared to the binary stars and the gas giant. However, test-computations with massive test-planets (up to an Earth-mass) showed the same dynamical behavior. The equations of motion were calculated numerically by means of the Lie series method using the *nine package* of Eggl (see Eggl & Dvorak 2010). Table 1 summarizes the different initial binary-planet configurations which were calculated for a time span between 10^6 and 5×10^6 years.

2.1. Influence of the secondary star

In a hierarchical four body problem gravitational perturbations like mean motion resonances (MMRs) and secular resonances (SRs) influence the architecture of a planetary system. Such perturbations are well visible in the various maps (Figs. 1, 2, 4, 5) which display the maximum eccentricity (max-e) of test-planets orbiting HD41004 A in the region between 0.15 and 1.3 au for various inclinations. The color code defines regions of different max-e values (from 0 to 1), where red marks the unstable zone. Most of these maps show

³In this context, Pilat-Lohinger & Funk (2010) studied the stability of this binary system using different published values of the eccentricity of HD41004 Ab to get upper limits for the binary’s eccentricity.

⁴The published value for $e_B = 0.4$ is 3.38 au (Roell et al. 2012) which is larger as they considered circular motion of the test-planets (according to Holman & Wiegert 1999).

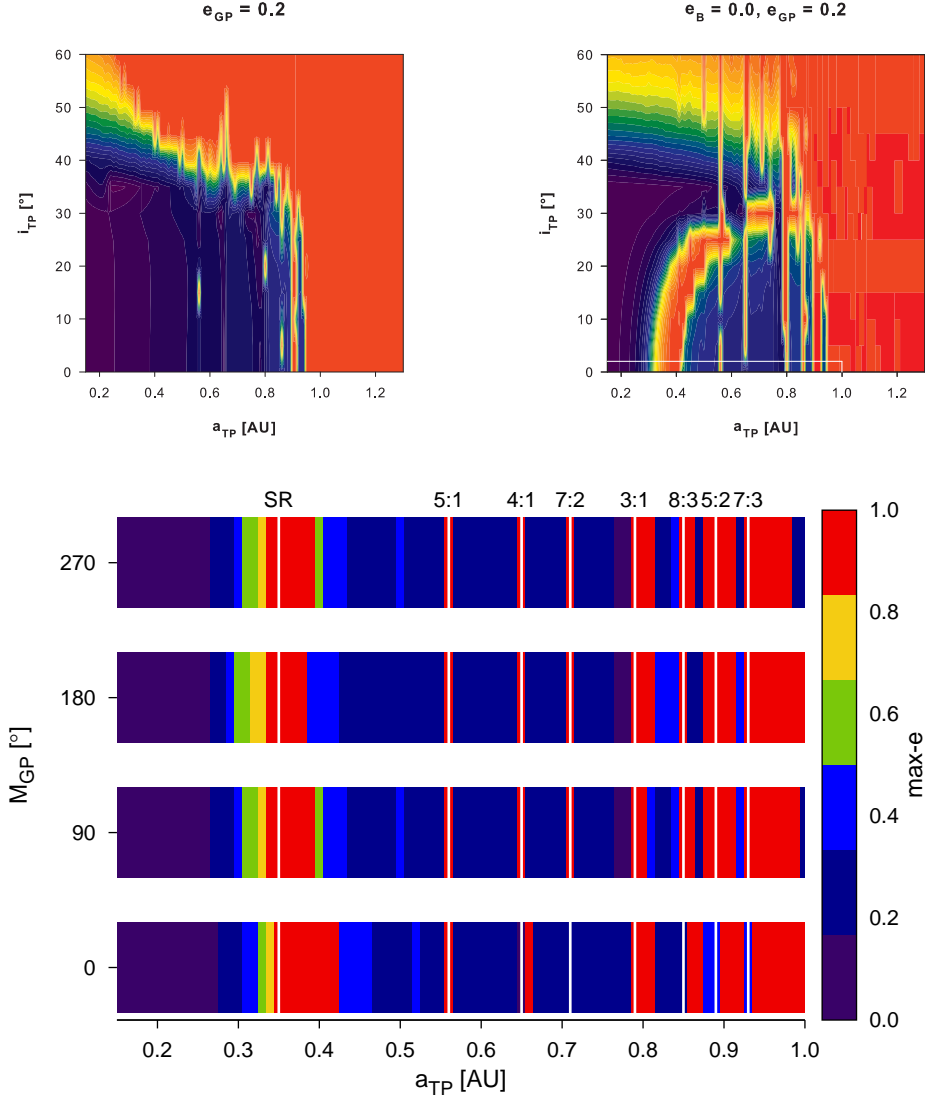


Fig. 1.— Max-e plots for (a) test-planets perturbed by a giant planet at 1.64 au (upper left panel) and (b) test-planets perturbed by the giant planet and a secondary (M-type) star at 20 au (upper right panel). The lower plot shows the max-e values for the area marked by the white rectangle in the upper right figure for various initial mean anomalies of the giant planet (M_{GP}) (see y-axis). The color code (which is the same in all max-e maps) indicates the different maximum eccentricities achieved by the test-planets over the whole computation time. Red labels the unstable area and purple indicates circular motion.

vertical straight lines indicating MMRs. In addition, a strong perturbation is visible by an arched red band within the stable area. We will show in section 4 that this perturbation is a linear SR. In certain maps the SR is not visible (see e.g. Figs. 4 right panels) because it is located either in the unstable (red) area or too close to the host-star.

The upper left panel of Fig. 1, does not show the SR as it represents the dynamics in the restricted three body problem where the secondary star was not taken into account. This plot indicates well known dynamical features of the restricted three body problem, like MMRs⁵ with respect to the giant planet (shown by the yellow spikes) and the cut-off of the stable region for inclinations $> 38^\circ$ caused by the so-called Kozai resonance Kozai (1962).

As soon as we add the secondary star at 20 au to the system a red arched band appears in the stable area (see Fig. 1 upper right panel) which arises from a perturbation of the giant planet and the secondary star (for details see the forthcoming section).

A comparison of the two upper panels of Fig. 1 shows that the extension of the stable area in a_{TP} is about the same which indicates that the border between stable and unstable motion is determined by the giant planet’s semi-major axis. The main differences of circumstellar motion in a binary system and the motion around a single star are the following:

- (i) In addition to MMRs a SR might appear under certain circumstances.
- (ii) The MMRs with respect to the giant planet are stronger and therefore better visible as the giant planet is perturbed by the secondary star leading to a fluctuation in e_{GP} .
- (iii) The border of unstable motion is shifted to higher inclinations ($i_{TP} > 60^\circ$) of the test-planets.

Moreover, the right panel of Fig. 1 shows that the region between the host-star and the SR is obviously not perturbed by the giant planet as the motion of the test-planets remains nearly circular during the whole computation. So we assume that this area would

⁵See also table 2.

provide best conditions for *dynamical habitability* as nearly circular planetary orbits will most probably be fully in the so-called habitable zone (HZ)⁶.

The white rectangle in this plot marks the planar motion of the test-planets for which we varied the initial mean anomaly of the giant (M_{GP}) and of the test-planet (M_{TP}) where the variation of the latter yield same results. The dynamical behavior in the labeled area for various M_{GP} is shown in the lower panel of Fig. 1. One can see that most of the resonances (indicated by the white vertical lines) appear even if we change the initial relative positions of the two planets. The 7:2 and the 5:2 MMRs are examples that are not visible for all calculated M_{GP} values.

3. Results of the numerical study

The initial conditions shown in table 1 yield in total 320 different binary-planet configurations for which we calculated max-e maps consisting of 1560 orbits each in the (a_{TP}, i_{TP}) plane. Here $a_{TP} = 0.15 \dots 1.3$ au and $i_{TP} = 0^\circ \dots 60^\circ$ denotes the semi-major axis and the inclination of the test-planet as shown in Figs. 2a-d. The color code indicates the different maximum eccentricities of the test-planets: from circular (purple) to highly eccentric motion (yellow). The unstable orbits are labeled by the red area. The four figures show the results for the same distance of the two stars ($a_B = 20$ au) and the same mass of

⁶The HZ is the region around a star where a terrestrial planet would have appropriate conditions for the evolution of life.

Table 2: MMRs in the HD41004 A system for $a_{GP} = 1.64$ AU:

MMR	2:1	3:1	4:1	5:1	5:2	5:3	6:1	7:1	7:2	7:3	7:4	8:3	9:2	9:4
Position[AU]	1.03	0.79	0.65	0.56	0.89	1.16	0.49	0.45	0.71	0.93	1.13	0.85	0.6	0.95

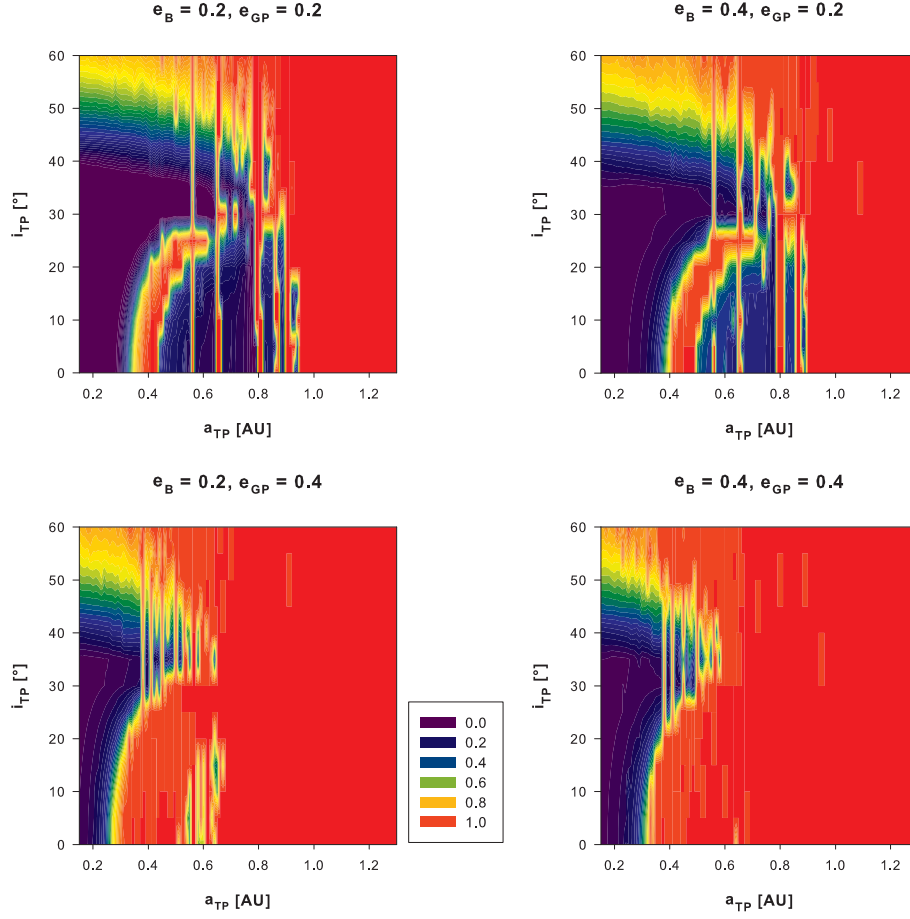


Fig. 2.— Max-e maps for planetary motion in the binary HD41004 where $a_B = 20$ au in all panels. Only the initial values of e_B and e_{GP} are changed between 0.2 and 0.4 as indicated in the title of each panel. The color code is the same as in Figs. 1.

the secondary star ($m_2 = 0.4m_{Sun}$). Only the initial eccentricities of the binary e_B and of the giant planet e_{GP} were varied between 0.2 and 0.4 for both.

3.1. Effect of e_B and e_{GP} on the dynamics of the test-planets

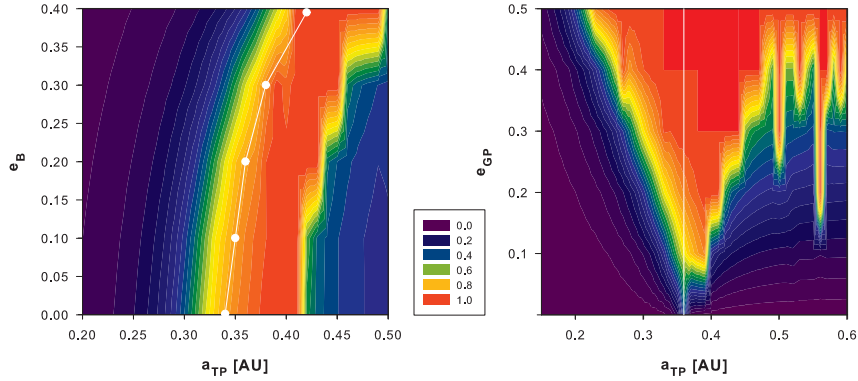


Fig. 3.— Max-e maps for HD41004 AB with $a_B = 20$ au. The left panel shows for a fixed value of $e_{GP}(= 0.1)$ the displacement of the perturbed area (red) when e_B (y-axis) is increased. Locations of the SR derived with our method are given by the white line of points. The right panel shows for a fixed $e_B(= 0.2)$ an enlargement of the perturbed area (red) when e_{GP} (y-axis) is increased, while the vertical white line represents the location of the SR calculated with our method.

A comparison of the different panels of Fig. 2(a-d) shows clearly that the planet’s eccentricity affects the stable area stronger than the binary’s eccentricity. An increase of e_{GP} shrinks the stable zone significantly, which can be seen when we compare either the two left panels or the two right panels of Fig. 2. Especially the area to the right of the arched red band is severely perturbed if e_{GP} is increased from 0.2 to 0.4. In the lower left panel of Fig. 2, one can see that the area of the SR is enlarged due to the higher e_{GP} . An increase in e_B from 0.2 to 0.4 indicates only a slight shift of this perturbation to the right

(compare the two upper panels of Fig. 2).

Due to these changes, we have plotted in Figs. 3 the extension of this perturbation for different eccentricities of the binary (left panel) and of the giant planet (right panel). These two panels confirm that changes in e_B will modify the location of the SR while an increase of e_{GP} enlarges the perturbed (red) area which is visualized in the right panel of Fig. 3 showing a V-shape for this perturbation. This phenomenon is well known for MMRs in such (a, e) maps.

3.2. Effect of a_B on the dynamics of the test-planets

A variation of the distance of the two stars (a_B) and the influence on the orbital behavior of the test-planets is given in Figs. 4(a-d). We show the results for two stellar separations: 30 au (left panels) and 40 au (right panels). The eccentricity of the binary is fixed to 0.2 and e_{GP} is either 0.2 (upper panels) or 0.4 (lower panels), respectively. A comparison with the equivalent results for $a = 20$ au (see Fig. 2, left panels) shows a significant shift of the SR towards the host-star. For $a_B = 30$ au, the arched red band is still visible but significantly reduced in the width. Moreover, in the upper left panel of Fig. 2 the color of the SR has changed to yellow with only a few red spots. This means that the orbits in this area are more stable but with strong periodic variations in eccentricity (up to $e = 0.8$). An increase in e_{GP} (see lower left panel) shows the following effects: (i) a significantly smaller stable region, (ii) an enhancement of the MMRs, (iii) an enlargement of the area of the SR and (iv) stronger perturbations within the SR.

A further increase of the stellar distance causes again a shift of the SR towards the host-star so that it moves out of the area we are studying. Only the yellow/red spot at $i_{TP} = 30^\circ$ indicates the existence of this phenomenon (see right panels of Fig. 4). A SR close to the host-star could cause periodic variations in eccentricity for close-in planets. How tidal

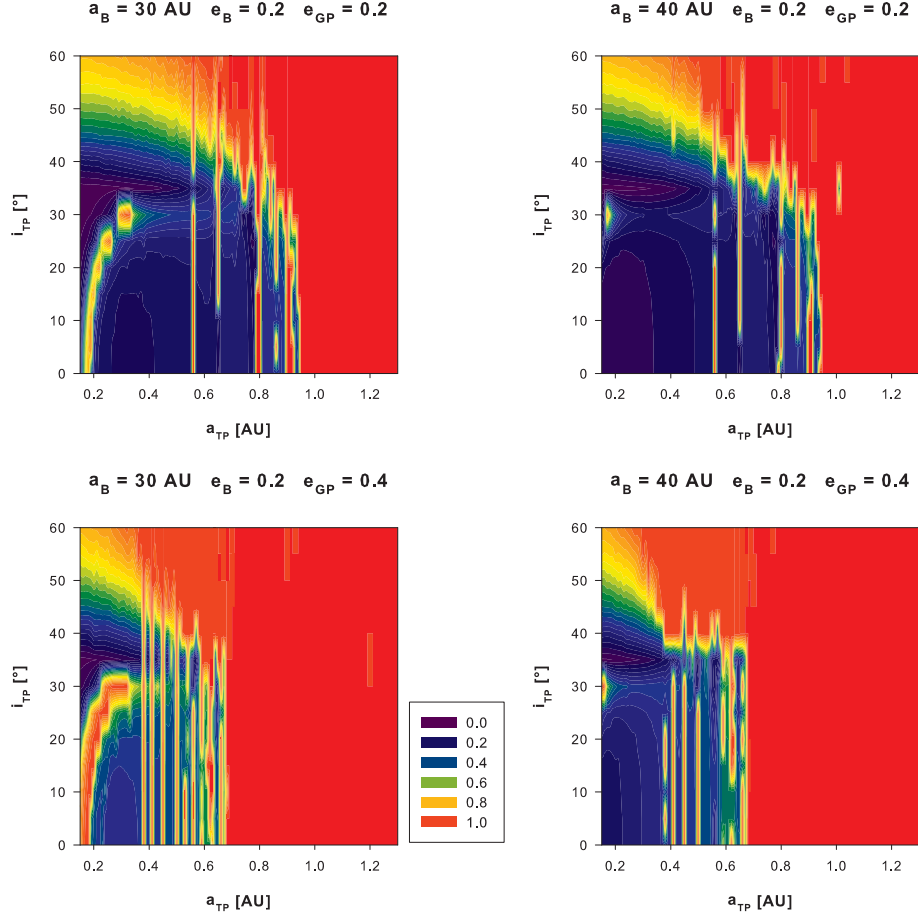


Fig. 4.— Max-e maps for different distances of the two stars and different e_{GP} , while e_B is fixed to 0.2. Left panels show the perturbations for the binary with $a_B = 30$ au and the right panels show the same for $a_B = 40$ au.

effects might influence the orbital behavior in addition could be an interesting aspect for a future study.

Figure 4.d (lower right panel) shows another new feature, namely the sharp border between stable and unstable motion at $i_{TP} = 38^\circ$ for the area perturbed by MMRs with respect to the giant planet (for a_{TP} from 0.4 to nearly 0.7 au). As this feature can be observed only for a low-mass secondary star we assume that in such a system this area is only affected gravitationally by the gas giant.

3.3. Effect of the secondary’s mass on the dynamics of the test-planets

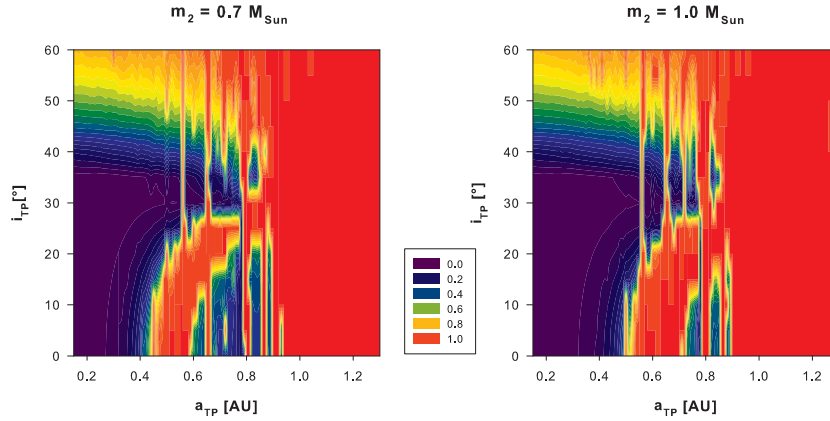


Fig. 5.— Max-e maps for test-planets around HD41004A perturbed by the giant planet at 1.64 au and the secondary star at 20 au. In the left panel, the secondary is a K-type star of 0.7 solar masses. In the right panel, the secondary is a G2-type star of 1 solar mass. The initial eccentricities are 0.2 for all massive bodies.

The influence of the mass of the secondary star is shown in Figs. 5(a,b). The two panels display the result of the same configuration as for the study of Fig. 2 upper left panel only the mass of the perturbing star at 20 au is increased. A comparison of these plots shows a shift of the SR to larger semi-major axes, i.e. in direction towards the giant

planet and the secondary star. In addition, we recognize an enlargement of the perturbed area due to the fact that a more massive secondary star has a stronger influence on the giant planet, so that the eccentricity of the giant planet is increased and the perturbed area will grow simultaneously.

4. Semi-analytical approach to locate a linear secular resonance

To explain the strong perturbation represented by the arched red band in various max-e maps (see e.g. Fig. 2a-d) we studied in detail the area between 0.2 and 0.6 au around HD41004A. In Fig. 6 (upper panel), we show the maximum eccentricity of the test-planets in planar motion in this region. Perturbations are indicated by higher values of max-e which is the case for the orbits at 0.53 au and 0.56 au and for all orbits in the area between 0.3 and 0.44 au. For this region, the lower part of Fig. 6 shows that the proper periods of the test planets are similar to the proper period of the giant planet which is given by the horizontal blue line in this panel. Consequently, this perturbed area is due to a linear secular resonance (1:1) where the frequencies of precession of the orientation of the orbits in space of the test-planets and of the giant planet are the same .

4.1. Numerical values for proper frequencies

To determine the proper frequencies of the orbits one needs long-term computations of the dynamical system where the integration time depends on the distance of the two stars, which is in our case about 20 au. For such a tight binary, we needed only calculations over some 10^6 years. Of course the computation time increases with a_B (as discussed in

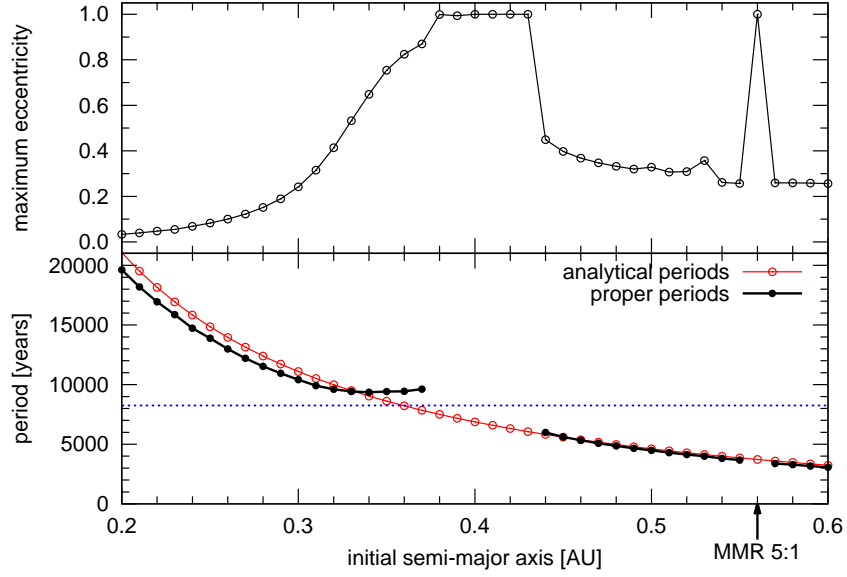


Fig. 6.— The upper part shows the maximum eccentricity of test-planets in planar motion in the region between 0.2 and 0.6 au. The lower part indicates the proper periods of the test-planets: black dots are the numerically determined values using a FFT method and red dots represent the analytical solution. The horizontal blue line indicates the proper period of the giant planet.

Bazsó et al. 2016).

The time evolution of the orbits was analyzed using the Fast Fourier Transform library FFTW of Frigo & Johnson (2005)⁷. In addition, we applied the tool *SigSpec* of Reegen (2007) for our orbital analysis where a Discrete Fourier Transform is used to decide whether a peak in the Fourier spectrum is not due to the noise in the signal. From the main frequency in the Fourier spectrum of an orbit we calculated the proper period. The results are shown by the black dots in the lower panel of Fig. 6. It is clearly seen that we could not determine the proper periods for orbits in the area between 0.38 and 0.43 au and at 0.56 au, i.e. for orbits with max-e= 1 (compare the two panels of Fig. 6). As the Fourier spectrum indicates a chaotic behavior for these orbits we could not determine the proper frequencies. In addition we tested the application of a secular perturbation theory for the determination of the proper frequencies of the test-planets.

4.2. Analytical values for proper frequencies

The well-known Laplace-Lagrange secular perturbations theory (see e.g. Murray & Dermott 1999) was used to derive an analytical solution for the proper frequencies. As this theory has been developed for studies in the solar system, it is restricted to low eccentricities and low inclinations. Nevertheless, we tested its application for the HD41004 binary system using an eccentricity of 0.2 for both, the binary and the giant planet. The massless test-planets were started with nearly zero initial eccentricities and inclinations. The secular frequency g was deduced according to the secular linear approximation (see e.g. Murray & Dermott 1999):

$$g = \frac{n}{4} \sum_{i=1}^2 \frac{m_i}{m_0} \alpha_i^2 b_{3/2}^{(1)}(\alpha_i) \quad (1)$$

⁷see <http://fftw.org/>

where $\alpha_i = a/a_i$ for $i = 1, 2$ and a_1, a_2, a are the semi-major axes of the giant planet, the secondary and the test-planet, respectively. m_1 and m_2 are the masses of the giant planet and the secondary and m_0 is the mass of the primary star. $b_{3/2}^{(1)}$ is a Laplace coefficient. According to Eq. 1, the value of g depends on the semi-major axes and the masses, which are all constant for a certain configuration. Therefore, the value of g is also constant for a given semi-major axis of a test-planet.

For calculations of proper frequencies usually a transformation to new variables⁸ (h, k) is made, where $h = e \sin \varpi$ and $k = e \cos \varpi$. Then, the general solution of the test-planets' motion is given by:

$$\begin{aligned} h(t) &= e_{free} \sin(gt + \Phi) - \sum_{i=1}^2 \frac{\nu_i}{g - g_i} \sin(g_i t + \Phi_i) \\ k(t) &= e_{free} \cos(gt + \Phi) - \sum_{i=1}^2 \frac{\nu_i}{g - g_i} \cos(g_i t + \Phi_i) \end{aligned} \tag{2}$$

where e_{free} and Φ are constants given by the initial conditions. The second part of the two Eqs. 2 varies with time as it depends on the secular solution. A secular resonance occurs in case $g_i \approx g$. In such a case, the forced eccentricity will increase rapidly to 1 leading to an escape or close encounter with another body of the system (as it can be seen in Fig. 6 in the area between 0.38 and 0.43 au. For details about this theory see e.g. Murray & Dermott (1999).

The analytically determined proper periods of the test-planets in the area between 0.2 and 0.6 au are shown by the red dots in the lower panel of Fig. 6. A comparison with the black dots in this figure shows the good agreement with the numerical values derived from

⁸We do not take into account variables associated with the inclination and node (usually called p, q in these variables), as we consider planar motion.

the Fourier analysis of the orbits. Especially in the region outside the secular resonance ($a_{TP} > 0.43au$) we have found perfect conformity of the two results. While for the area closer to the host-star the proper periods of the analytical solution are slightly larger.

4.3. The location of the linear SR – a new semi-analytical method

As the analytical solution represents a good approximation for the proper periods of the test-planets, the position of the SR ($= a_{SR}$) can be determined from the intersection of the red and the blue lines in the lower panel of Fig. 6. Consequently, we need only one numerical computation of the dynamical system in order to determine a_{SR} . The application of this semi-analytical method to the HD41004 binary using different eccentricities for the binary and the giant planet is shown in Fig. 7 where one can recognize a strong shift of a_{SR} for a change of e_B from 0.2 to 0.4, which is visible by a comparison of either the two (horizontal) full lines or the two dashed lines. The different grey shades indicate different eccentricities of the binary ($e_B = 0.2$ see the dark grey lines and $e_B = 0.4$ the light grey lines). While different eccentricities of the giant planet are shown by different line styles (the full line represents the result for $e_{GP} = 0.2$ and the dashed line for $e_{GP} = 0.4$). A comparison of the proper periods for two different e_{GP} 's of a certain e_B shows only a small shift in a_{SR} .

The intersection of the curve representing the analytical solution for the proper periods of the test-planets (i.e. the black curve in Fig. 7) with the numerically determined proper period of the giant planet (i.e. the horizontal lines for the different e_B and e_{GP} in Fig. 7) defines the position of the linear SR but not the width which can be quite large in case of high eccentric motion of the giant planet (as shown in Fig. 3 right panel). The vertical white line indicated the location of the SR.

One can notice that this location is not centered in the V-shape of the perturbed area.

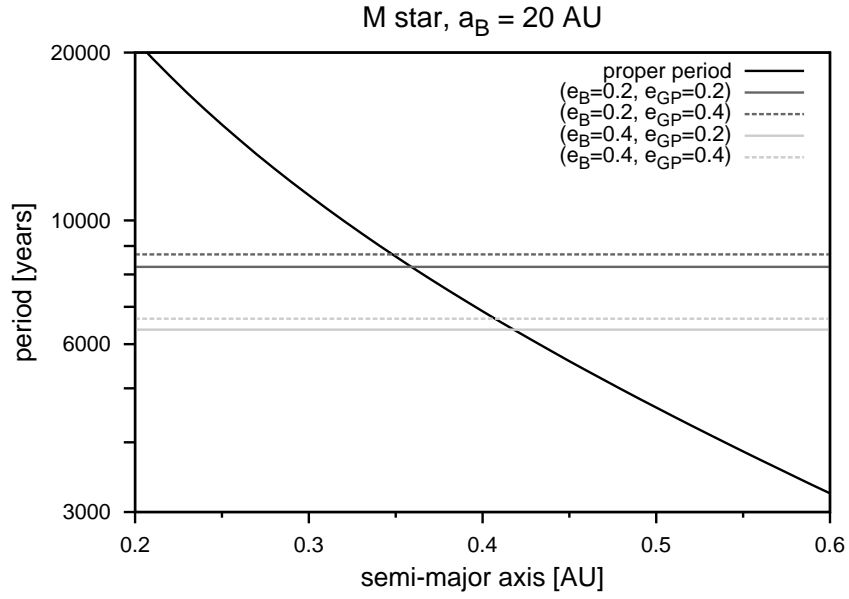


Fig. 7.— The semi-analytical method applied to the HD41004 binary using different eccentricities (0.2 and 0.4) for the giant planet and for the binary as shown by the legend. The black curve represents proper periods of the test-planet which were analytically determined. The different horizontal lines show the proper period of the giant planet in the various binary configurations. The location a_{SR} is defined by the intersection of a horizontal line with the black curve.

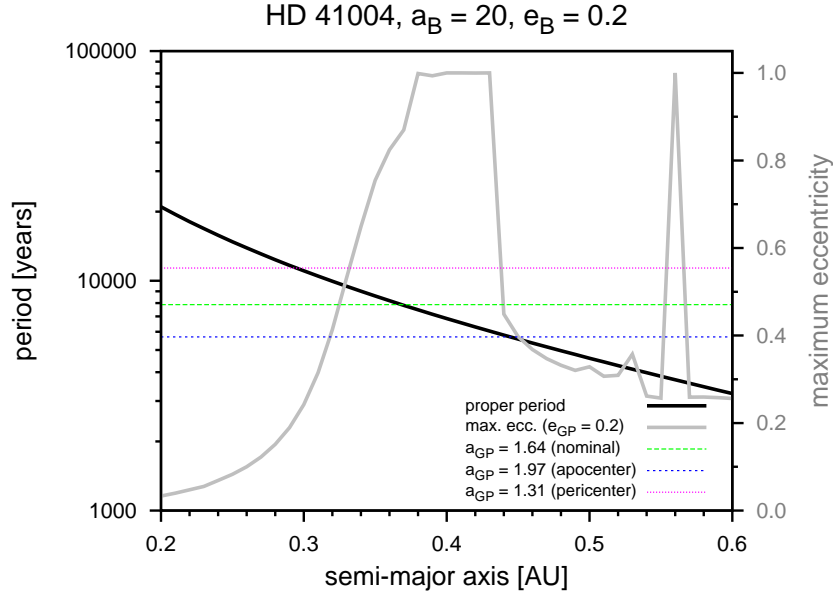


Fig. 8.— The application of the semi-analytical method to the apo- and peri-center positions of the giant planet in the HD41004 binary. The proper period of the giant planet derived for these positions are shown by the blue and magenta lines for the apo-center and peri-center, respectively. The green line labels the proper period for the giant planet for a_{GP} . The black curve shows the proper periods of the test-planets and the light grey curve marks the maximum eccentricities of the test-planets. The intersection of the black curve (i) with the green line indicates a_{SR} ; (ii) with the blue line marks the outer border of the linear secular resonance and its inner border is defined by (iii) the intersection with the magenta line. For more details see the text.

It is more or less the inner boundary of the perturbed area. Moreover, we recognized that the location a_{SR} will not change significantly when increasing the giant planet’s eccentricity. Only the width will increase as indicated by the V-shape in the right panel of Fig. 3. The two plots show that the eccentricity of the binary is important for the location of the SR while the eccentricity of the giant planet is responsible for the extension of the SR. To determine the width of the SR, we replaced a_{GP} by the peri- and apo-center distances⁹ of the giant planet and calculated the proper frequency of the giant planet for these positions. The result is shown in Fig. 8 by the horizontal lines where the green line labels the proper period for a_{GP} , the blue line shows the result for $a = a_{apocenter}$ and the magenta line represents the result for $a = a_{pericenter}$. Looking at the intersections of these lines with the black curve (representing the proper periods of the test-planets) one can see from the crossing point of the blue line (at 0.445 au) that the apo-center position defines well the outer rim of the SR. This is confirmed by the grey line representing the maximum eccentricities of the test-planets which shows a sudden change in max-e in this area. However, the intersection point of the magenta line is not recognized immediately as inner border of the SR. Only if we examine this positions (i.e. 0.295 au) more closely we notice that at this intersection the max-e value starts to be larger than e_{GP} and it grows smoothly towards 1 when approaching a_{SR} . The resulting shape of max-e curve seems to be significant for regions where SRs are acting, as this shape was also found in a study by Malhotra (1998).

The application of our method to the apo- and peri-center positions of the giant planet determined obviously quite well the width of the SR (at least for an eccentricity of 0.2 for the binary and the giant planet).

⁹For e_B and $e_{GP} = 0.2$: the apo-center is at 1.97 au and the peri-center is at 1.31 au

4.4. A study of different binary configurations of HD41004

The successful application of our newly developed semi-analytical method motivated us to study the different binary-planet configurations of HD4104 AB of section 3 again with the aid of this method to verify if we obtain similar features as in our numerical investigation. Therefore, we varied (i) the semi-major axis of the binary from 10 au to 40 au, (ii) the eccentricities of the binary and of the giant planet using either 0.2 or 0.4, and (iii) the mass of the secondary star (using 0.4, 0.7 and 1 solar mass). For the resulting 48 binary-planet configurations we determined a_{SR} applying our method. The results of this study are summarized in table 3. This overview shows clearly that an increase of the secondary’s mass from 0.4 (M-type star) to 1 solar mass (G-type star) causes an outward shift of the SR to larger semi-major axes for a binary configuration. While an increase of the distance between the two stars (here from 10 to 40 au) indicates an inward shift of the SR. As already pointed out in the previous section, table 3 shows clearly that a change of e_B leads to a stronger displacement of the secular resonance than a change in e_{GP} . A comparison with the numerical computations of the previous sections shows that the results of both studies are in good agreement which demonstrates the accurateness of this method.

5. Conclusion

We studied the planetary motion around one stellar component of a binary system. As dynamical model we used binary configurations resembling the HD41004 AB system where a planet (HD41004 Ab) has been detected at 1.64 au (Zucker et al. 2003, 2004). The aim of this work was to continue and improve the study of Pilat-Lohinger (2005) and to figure out in detail the influence of a secondary star on the motion of test-planets in the area between 0.15 and 1.3 au.

First we showed in a purely numerical approach the perturbations due to the giant planet

Table 3: Location of the SR (a_{SR}) for different HD41004 binary configurations:

	$e_B = 0.2$		$e_B = 0.4$	
a_B [au]	$e_{GP} = 0.2$	$e_{GP} = 0.4$	$e_{GP} = 0.2$	$e_{GP} = 0.4$
a_{SR} [AU] for a M-type star secondary:				
10	0.96	0.94	1.08	–
20	0.36	0.35	0.42	0.41
30	0.17	0.16	0.20	0.19
40	0.10	0.09	0.11	0.11
a_{SR} [AU] for a K-type star secondary:				
10	1.07	1.08	–	–
20	0.50	0.48	0.58	0.56
30	0.24	0.23	0.28	0.27
40	0.14	0.13	0.16	0.15
a_{SR} [AU] for a G-type star secondary:				
10	1.25	1.25	–	–
20	0.60	0.58	0.68	0.67
30	0.30	0.29	0.35	0.34
40	0.18	0.17	0.21	0.20

and the secondary star. The max-e plots display the MMRs and SRs where the latter changed place when we varied the orbital parameters of the binary. A similar behavior has been found by Pilat-Lohinger (2005) for a variation of the giant planet’s semi-major axis. Depending on the binary-planet configuration the secular resonance can influence also the motion in the habitable zone. Moreover, our system configurations showed that test-planets with semi-major axes $a < a_{SR}$ (i.e. the semi-major axis of the secular resonance) move on nearly circular orbits and provide therefore, best conditions for habitability from the dynamical point of view.

In the second part of this investigation, we developed a semi-analytical method which allows a fast determination of a_{SR} . Only one numerical integration of the binary-planet configuration is needed to determine the proper frequency of the giant planet. While the test-planets’ proper frequencies were taken from the analytical solution of the Laplace-Lagrange secular perturbation theory. The intersection of both results defines the location of the SR.

We showed that the results for the binary HD41004 AB of a purely numerical study and of our semi-analytical approach are in good agreement. Further applications of this method to tight binary star systems with a detected planetary companions in circumstellar motion are shown by Bazsó et al. (2016).

The authors want to acknowledge the Austrian Science Fund (FWF) for the financial support of this work which was carried out in the framework of the projects P22603-N16 and S11608-N16 (a sub-project of the NFN Project “Pathways to Habitability”). EP-L wants to thank Dr. P. Robutel from IMCCE (Paris, France) for fruitful discussions about frequency analysis of planetary motion. Finally, we thank the unknown referee for helpful suggestions to improve the paper.

REFERENCES

- Bazsó, Á., Pilat-Lohinger, E., Eggl, S., Funk, B., Bancelin, D. 2016, in prep.
- Benest, D. 1988, A&A, 206, 143
- Benest, D. 1988, CMDA, 43, 47
- Benest, D. 1989, A&A, 223, 361
- Benest, D. 1993, CMDA, 56, 45
- Black, D.C. 1982 AJ, 87, 1333
- Cochran, W.D., Hatzes, A.P., Endl, M., Pauson D.B., Walker G.A.H., Campbell, B., Yang, S., 2002, Astron. Astrophys. Suppl. Ser. 34, 916
- Duquennoy, Mayor, M., 1991, A&A, 248, 485
- Dvorak, R., 1984, CMDA, 34, 369
- Dvorak, R., 1986, A&A, 167, 379
- Dvorak, R., Froeschlé, C., Froeschlé, Ch., 1989, A&A, 226, 335
- Dvorak, R., Pilat-Lohinger, E., Funk, B., Freistetter, F., 2003, A&A, 398, L1
- Eggl, S., Dvorak, R. 2010, in LNP 790, Berlin Springer Verlag, eds. J. Souchay & R. Dvorak, 431
- Frigo, M., Johnson, S.G. 2005, Proceedings of the IEEE 93, 216 special issue on “Program Generation, Optimization, and Platform Adaptation”
- Graziani, F., Black, D.C. 1981, ApJ, 251, 337
- Harrington, R. S., 1977, ApJ, 82, 753

- Holman, M.J., Wiegert, P.A. 1999, *AJ*, 117, 621
- Kozai, Y. 1962, *AJ*, 67, 591
- Malhotra, R. 1998, *ASP Conference Series*, 149, eds. D. Lazzaro et al., 37
- Murray, C.D., Dermott, S.R. 1999, *Solar system dynamics*, Cambridge University Press
- Pilat-Lohinger, E., Dvorak, R., 2002, *CMDA*, 82,143
- Pilat-Lohinger, E., Funk, B., Dvorak, R., 2003, *A&A*, 400, 1085
- Pilat-Lohinger, E. 2005, in *IAU Colloq. 197: Dynamics of Populations of Planetary Systems*, eds. Z. Knežević & A. Milani, 71
- Pilat-Lohinger, E., Funk, B. 2010, in *LNP*, 790, Berlin Springer Verlag, eds. J. Souchay & R. Dvorak, 481
- Pilat-Lohinger, E. 2011, *IAU Symposium 282: From interacting binaries to exoplanets: Essential modeling tools*, eds. M.T. Richards & I. Hubeny, 539
- Rabl, G., Dvorak, R. 1988, *A&A*, 191, 385
- Raghavan, D., M Alister, H. A., Henry, T. J., et al. 2010, *ApJS*, 190, 1
- Queloz, D., Mayor, M., Weber, L., Blicha, A., Brunet, M., Confino, B., Naef, D., Pepe, F., Santos, N., Udry, S. 2000, *A&A*, 354, 99
- Reegen, P. 2007, *A&A*, 467, 1353
- Roell, T., Neuhäuser, R., Seifahrt, A., Mugrauer, M. 2012, *A&A*, 542, A92
- Tokovinin, A. 2014, *AJ*, 147, 87
- Zucker S., Mazeh T., Santos N.C., Udry S., Mayor M. 2003, *A&A*, 404, p.775

Zucker S., Mazeh T., Santos N.C., Udry S., Mayor M. 2004, A&A, 426, p.695